Available online at www.sciencedirect.com

ScienceDirect

Ciência & Tecnologia dos MATERIAIS

http://ees.elsevier.com/ctmat

Ciência & Tecnologia dos Materiais 28 (2016) 138–146

Viscoelastic behaviour and modelling of nano and micro TiO_2 powder-epoxy resin composites

G.C. Papanicolaou*, L.C Kontaxis, A.E. Manara

The Composite Materials Group, Department of Mechanical and Aeronautics Engineering, University of Patras, Patras, GR-26500, Greece

Abstract

Epoxy resin composites reinforced with different weight fractions of TiO_2 micro-particles 0.2μm in size (1%, 5%, 10%, 15%wt) and of TiO_2 nano-particles 21nm in size (0.5%, 1%, 3%wt) were manufactured. The quasi-static mechanical properties of both nano-composites and micro-composites were investigated and compared through tensile testing. The experimental results were predicted and the degree of matrix-particle adhesion and particle dispersion were evaluated, by the Property Prediction Model (PPM) developed by the first author. The composites were also subjected to creep-recovery tests as well as to relaxation tests in order to investigate their viscoelastic behaviour. The experiments were carried out at different filler-weight fractions and loading conditions. Non-linear viscoelastic behaviour was observed in all cases and appropriate models were applied in order to describe, and/or predict the viscoelastic behaviour of all materials tested. A fair agreement between experimental results and theoretical predictions was observed for both viscoelastic and static results.

Keywords: viscoelastic; nano; micro; TiO_2; titania.

1. Introduction

Over the last two decades a large amount of research concerning nanotechnology and its application on composite materials has been conducted. Nanoparticles embedded in polymer matrix have attracted increasing interest because of the unique mechanical, optical, electrical and magnetic properties displayed by nano-composites. Unlike bulk materials, because of the nanometre size of the embedded particles, their physicochemical characteristics differ significantly. The composites produced from the combination of the host polymeric matrix and the nanoparticles possess properties of both materials [1]. Consequently epoxy nano-composites exhibit a wide range of positive characteristics such as dielectric behaviour, thermal stability, corrosion resistance, mechanical performance, and excellent tribological properties [2-6].

Early findings have shown that the size of the embedded particles in polymeric matrices is a very important factor affecting the overall behaviour of the composite [7,8]. However, in some cases, it was found that particle size does not affect Young's modulus [9-13] up to a certain threshold, on the order of 30 nm [14-16]. Nevertheless, the magnitude of this critical particle size cannot be predicted, for it depends on the particle and matrix nature and particle/matrix adhesion efficiency [17].

Titanium dioxide is being used in several applications such as energy converter in solar cells, electrode material in lithium batteries, coatings, and membranes for water filtration and gas sensors [18-22]. Scientists have also manufactured TiO_2 nano fibres in order to improve the photocatalytic properties of the existing materials [23]. In addition, TiO_2 nanoparticles have been added to lubricants to increase the load capacity of a journal bearing [24]. Finally, TiO_2 has been investigated as material used in many biomedical applications [25]. In literature, TiO_2 nano- and micro-composites have been characterised by tensile,

* Corresponding author.

E-mail address: gpapan@mech.upatras.gr (G.C. Papanicolaou)

http://dx.doi.org/10.1016/j.ctmat.2016.02.005

flexural, pull-off and abrasion tests and it was found that nano-particles improved the properties under test more efficiently than their micro counterparts [26,27]. The present study investigates the effect of the size of TiO_2 micro- and nano-particles on the quasi-static and viscoelastic properties of epoxy/TiO_2 composites.

2. Materials and methods

2.1. Materials

Epoxy resin RenLam CY219 (Bisphenol A) combined with a curing agent HY 5161 (Diamine) at a ratio 2: 1 by weight was used as matrix material. Gelling time was 24 hours at 50 ºC, and mass density of cured polymer 1.1 gcm^{-3}. Viscosity of the system CY219 and HY 5161 was 1-1.2 Pas at 25ºC. Titanium(IV) oxide nano-powder supplied by Sigma-Aldrich was used, with an average particle size of 21 nm, specific surface area 35-65 m^2g^{-1}, mass density 4.26 gcm^{-3}, and purity of titania nanoparticles ≥ 99.5% , exposed for thermal treatment at 50ºC for 24 hours to ensure discard of H_2O molecules absorbed by titania nanoparticles. Titanium Dioxide Rutile 2902 micro-particles supplied by Vellis Chemicals were used, with an average particle size of 0.2 μm and mass density 4.1 gcm^{-3}, also exposed for thermal treatment at 50ºC for 24 hours. The physical properties of TiO_2 micro- and nano-particles are presented in Table 1 as given both by the manufacturers' datasheets and literature [28].

2.2. Micro-particulate specimens manufacturing

The resin was placed first in an oven for 10 minutes at 40ºC in order to decrease its viscosity. Next, titanium dioxide was placed in the oven at 50ºC for 24 hours in order to dry, as mentioned above. Polymer resin and TiO_2 micro-particles 0.2μm in size (1%, 5%, 10%, 15%wt) were carefully mixed by means of an electrical stirrer, in proper quantities, in order to achieve uniform distribution of the fillers into the matrix. Then, the mixture was placed in a vacuum chamber for 5–6 min to reduce the amount of entrapped air. The mixture was then poured in a proper metallic mould and subsequently cured in an oven at 50 ºC for 24 h.

2.3. Nano-particulate specimens manufacturing

The resin was placed in an oven for 10 minutes at 40 ºC in order to decrease its viscosity. Titania nanoparticles were added to the hardener in a plastic beaker and mixed by means of an electrical stirrer for preliminary dispersion. The mixture was placed in the sonicator for 5 minutes at 10 kHz. In order to avoid temperature rise during sonication, external cooling was employed by submerging the mixing beaker into a mixture of ice and salt water. The beaker with the resin was also submerged into a mixture of ice and salt water and the TiO_2-hardener system was added in the resin and mixed via an electrical stirrer until homogeneity was achieved. The final mixture was placed in a vacuum chamber for 5–6 min to reduce the amount of entrapped air.
Bandelin Sonopuls HD 2200 sonicator homogenizer was used for dispersion of the TiO_2 nano-particles. The maximum power output was 200 Watts applied at a maximum frequency of 20 kHz using a 13mm diameter titanium flat tip.

Table 1. Physical properties of TiO_2 micro- and nano- particles.

	TiO_2 Nano-Particles	TiO_2 Micro-Particles
Particle size	21 nm	0.2 μm
Molar Mass	79.866 g/mol	79.866 g/mol
Specific Surface Area	35-65 m^2/g (BET)	12 m^2/g (BET)
Odour	odourless	odourless
Density	4.26 g/cm^3	4.1 g/cm^3
Melting point	1843 °C	1843 °C
Boiling point	2972 °C	2972 °C

3. Experimental characterization

The degree of dispersion of TiO_2 particles into the epoxy matrix was checked by means of a Scanning Electron Microscopy (SEM device, Model Zeiss SUPRA 35VP) in the absence of any conductive sputtering.
The tensile properties of the materials manufactured were determined in accordance with ASTM D0638-03 with a displacement rate of 5mm/min (Instron 4301).
The tensile stress relaxation tests were conducted at three different elongation levels (1mm, 1.5mm and 2mm) with applied displacement rate of 50mm/min (Instron 4301). Each experiment lasted for 90 minutes. The relaxation specimens were manufactured in accordance with ASTM D0638-03.
The tensile creep-recovery tests were conducted at three different stress levels of 3.2MPa, 6.4MPa and

9.6MPa. Each experiment lasted 6 hours while the overall time of experiment was equally divided between the tensile creep and the tensile creep-recovery test (3 hours for each stage). All specimens were tested by means of a customized arm lever creep testing machine, and their dimensions were 165x20x2.5 mm^3.

4. Theory

4.1. Property prediction model (PPM)

Property Prediction Model (PPM) is a semi-empirical model developed by the first author and is used to predict the property variation with filler-volume fraction. It is the improved version of the Modulus Prediction Model (MPM) already presented in [29, 30] after it was found that it can predict more material properties in addition to the elastic modulus [31]. The PPM model is described by the following Equation 1:

$$P_c = (\lambda - \kappa) P_f V_f^2 + \kappa(P_f - P_m) V_f + P_m \quad (1)$$

where Pc is the current property value, P_f and P_m is the filler and matrix property value respectively, λ is dispersion parameter and κ the adhesion parameter. Finally, the filler volume fraction is denoted by V_f. Knowing only two experimental points, specifically one at a very low filler concentration and a second one at a high filler concentration, one can determine the parameters κ and λ. Then, through Equations 2 and 3 estimations for the degree of adhesion, K, and the degree of dispersion, L, can be calculated as:

$$K = \left|\frac{\kappa}{2-\kappa}\right| \quad (2) \quad \text{and} \quad L = \left|\frac{\lambda}{2-\lambda}\right| \quad (3)$$

4.2. Residual property model (RPM)

The RPM model, is a model developed by the CMG group, at the University of Patras, and it is used for the prediction of the residual property value of polymers and polymer-matrix composites, after damage. As it has already been shown, the model gives accurate predictions for the residual materials properties variation irrespectively of the cause of damage and the type of the material considered at the time [29, 32, 33].

The final expression for the RPM model is:

$$\frac{P_r}{P_0} = s + (1-s)\cdot e^{-SM} \quad (4)$$

where P_r is the residual after damage property value and P_0 is the value of the same property for the undamaged material. Also M is a specific parameter, characteristic of the type of the damage source and which, in the case of relaxation is given by Eq.(6).

Furthermore,

$$s = \frac{P_\infty}{P_0} \quad (5) \quad \text{and} \quad M = \frac{t}{\tau_{rel}} \quad (6)$$

where P_∞ is the material property value when under damage saturation condition. Finally, by τ_{rel} is denoted the relaxation time of the material tested.

4.3. Four element model (Burger's Model)

The four element model or Burger's model is the in series combination of a Maxwell model and a Voigt model and is mainly applicable only to linear viscoelastic behaviour conditions. The constitutive equation of the model for the creep is [34]:

$$\varepsilon(t) = \frac{\sigma_0}{E_1} + \frac{\sigma_0}{\eta_1}\cdot t + \frac{\sigma_0}{E_2}\cdot(1-\exp(-E_2\cdot t/\eta_2) \quad (7)$$

Also, the constitutive equation of the model for recovery is [34]:

$$\varepsilon(t) = \frac{\sigma_0}{\eta_1}\cdot t_1 + \frac{\sigma_0}{R_2}\cdot(\exp(R_2\cdot t_1/\eta_2)-1)\cdot\exp(-R_2\cdot t/\eta_2) \quad (8)$$

where t_1 is the time instant where the recovery of the material starts, and $t>t_1$.

5. Results and discussion

5.1. Scanning electron microscopy (SEM)

In Fig. 1a and 1b, the surface topography of micro- and nano-epoxy/TiO_2 composites can be observed through scanning electron microscopy. The uneven surface of the specimens can be attributed to the slice mark caused during sample preparation. The SEM image presented in Fig. 1a corresponds to the highest TiO_2 micro-particles weight fraction (15%wt). Although the micro-particles distribution looks fairly homogeneous, the formation of aggregates can be detected as well, since this is a critical weight fraction, above which TiO_2 micro-particles aggregation is inevitable. Fig. 1b shows the 3%wt TiO_2 nano-composite. It is very challenging to observe the nano-particles, due to their extremely small size (21 nm), however the presence of large visible agglomerations

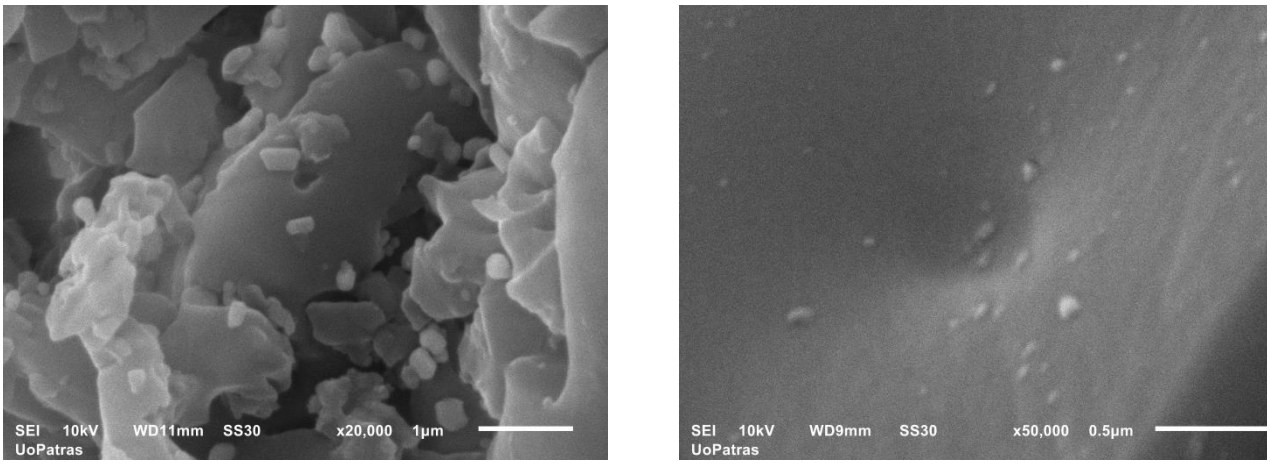

(a) **(b)**

Fig. 1. SEM photo-micrographs of TiO_2/epoxy composites at: (a) 15 %wt micro-particles, and (b) 3%wt nano-particles of TiO_2.

was not observed, concluding that a satisfactory particle distribution was achieved.

5.2. Tensile characterization

The materials manufactured were then characterized in tensile testing with a displacement rate of 5mm/min in an Instron 4301 universal testing machine. The variation of the tensile modulus of the composites investigated with the filler weight fraction and filler size is shown in Fig. 2. Also, the PPM modulus predictions were plotted together with respective experimental data in the same diagram. It can be seen that the model predicts extremely well the variation of the tensile modulus as a function of the filler-weight fraction, for both micro- and nano- TiO_2 composites. The deviation between experimental and theoretical values never exceeded 3.13%. A 0.33 degree of adhesion, K, was found for the nano-composites while a 0.56 degree of adhesion for the TiO_2/epoxy micro-composites was calculated. Taking into account that a value of K=1 corresponds to perfect adhesion conditions, the above calculated values seem to be quite acceptable. On contrary, the degree of dispersion, L, is vastly different when comparing the micro- and nano-composites respective values. More precisely, the model predicts a medium value of 0.48 for the degree of micro-composites, while it predicts a very high degree of dispersion value equal to 0.95 for the nano-composites. Taking into account that a value of L=1 corresponds to perfect dispersion conditions, these findings show that the conditions followed for the nano-composites manufacturing led to a perfect dispersion of nano-fillers into the polymeric matrix and this is better observed in Fig. 1b.

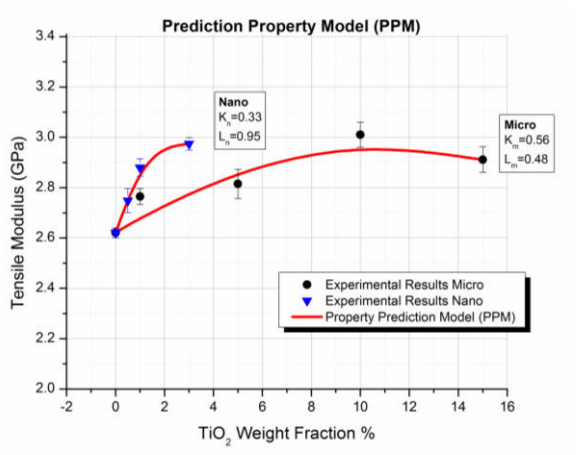

Fig. 2. Comparison between experimental values and theoretical predictions as derived from the property prediction model (PPM) for the tensile modulus of the micro- and nano- TiO_2 particle-epoxy matrix composites investigated.

At this point it is worth mentioning that modulus increase rate with TiO_2 particle concentration for nano-composites is almost double the respective rate of increase corresponding to micro-composites. This is attributed to the higher surface contact area of nano-composites as compared to the respective area for micro-composites corresponding to the same filler concentration.

5.3. Tensile creep-recovery results

In Fig. 3 to 5 the cumulative strain-time diagrams for the creep and the creep-recovery behaviour are given, for all weight fractions, concerning both micro- and nano- TiO_2 composites. The manufactured composites were tested in creep under 3.2 MPa, 6.4 MPa and 9.6 MPa stress loadings.

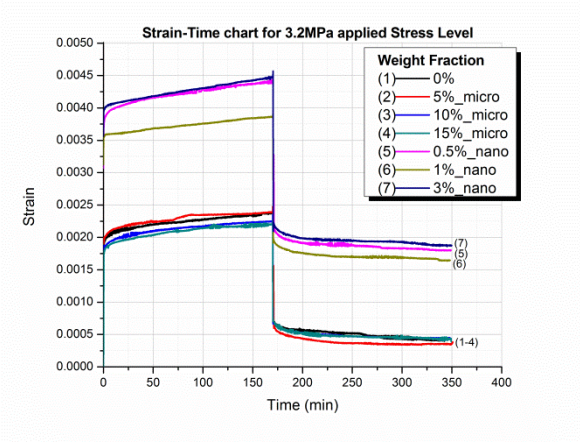

Fig. 3. Strain versus time creep-recovery curves, for 3.2 MPa applied stress level, and for different TiO_2 particle sizes and weight fractions.

At the lowest stress level applied (i.e. 3.2 MPa), a big difference between the nano- and micro- TiO_2 composites strain levels can be observed (Fig. 3). This phenomenon can be attributed to the sensitivity that the nano-particles exhibit because of their increased specific surface area.

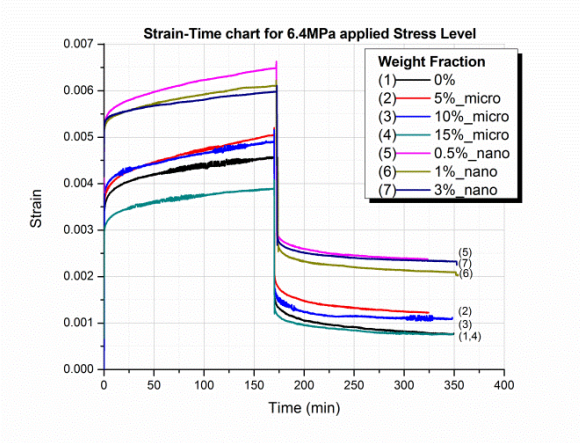

Fig. 4. Strain versus time creep-recovery curves, for 6.4 MPa applied stress level, and for different TiO_2 particle sizes and weight fractions.

Due to this increased contact area between the epoxy matrix and the TiO_2 nano-particles the applied stresses can be transferred easier to the particle, even at low stress levels. On the contrary the micro-particles lack that sensitivity, due to the lower contact area; therefore there is no such a strain difference between the strain levels obtained for the micro- TiO_2 composites and that of the pure epoxy resin. As the stress level applied increases, the obtained strain difference between the nano- and the micro- TiO_2 composites decreases as can be seen in Fig. 4. As the stress level increases, the ability of the micro-composites interphase to convey the developed stresses on the particles increases as well. This is because the developed stresses are high enough and the sensitivity level the nano-particles provide is not of great significance after a certain stress threshold.

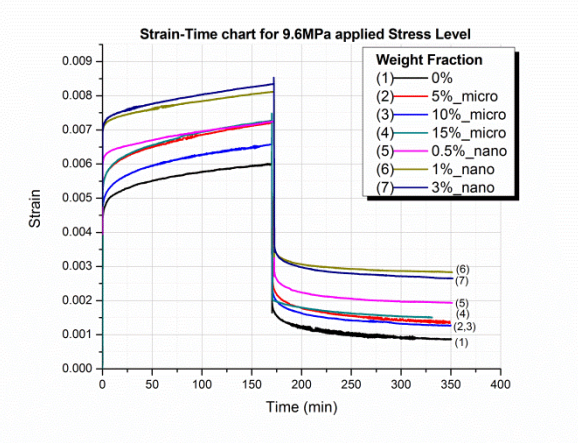

Fig. 5. Strain versus time creep-recovery curves, for 9.6 MPa applied stress level, and for different TiO_2 particle sizes and weight fractions.

Finally, at very high stress level the behaviour of both micro- and nano- TiO_2 composites appears to be the same, in a way such that the particle size seems not to affect the viscoelastic behaviour of the materials significantly anymore (Fig. 5). We can safely assume that after a certain upper stress threshold the strain gap between micro- and nano- TiO_2 composites is totally eliminated. This upper stress threshold can be assumed to be close to the linear/non-linear viscoelastic transition region. Evidence for such behaviour is the isochronous curves shown in Fig. 6 and which are of non-linear character.

5.4. Tensile stress relaxation results

In Fig. 7 to 9 the cumulative stress-time diagrams for the relaxation behaviour of both micro- and nano-TiO_2 composites and for the different filler weight fractions are considered. The manufactured

composites were tested for 0.83%, 1.25% and 1.66% applied strain levels.

Fairly high strain levels were chosen for the relaxation experiments in order to reach with certainty the non-linear viscoelastic region and observe the behaviour of the manufactured materials under these conditions.

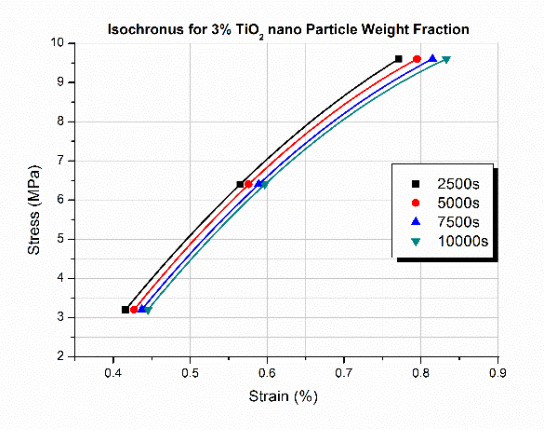

Fig. 6. Isochronous curves of epoxy-TiO_2 nano-composites with 3%wt particle concentration and for different values of applied stress levels up to 9.6MPa.

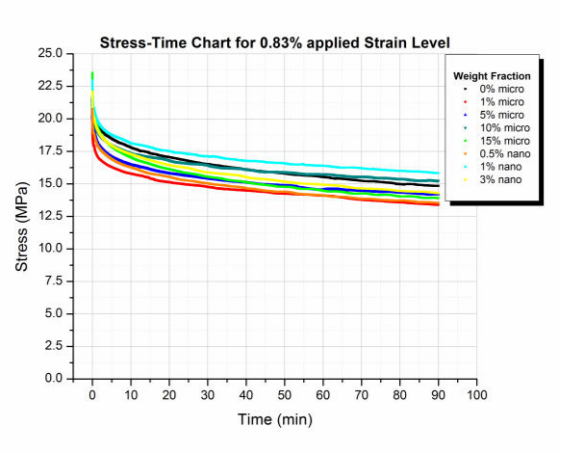

Fig. 7. Stress versus time relaxation curves, for 0.83% applied strain level, and for different TiO_2 particle sizes and weight fractions.

Another reason for the choice of these high imposed strain levels was the application of the RPM model on the obtained results. The goal was to confirm its effectiveness in predicting the non-linear viscoelastic behaviour, since its success has already been confirmed for predicting linear viscoelastic behaviour [30]. By examining Fig. 7 to 9, the intense plasticity of the matrix can be observed. Due to this fact it appears as if the particles do not affect the relaxation behaviour of the composites manufactured. In these high strain levels we tackle the same phenomenon we observed in the creep-recovery experiments for the highest stress level applied (i.e. 9.6MPa).

Evidence to the fact that the test samples have already surpassed the non-linear viscoelastic region exhibiting non-linear viscoelastic behaviour is given by the respective isochronous curves shown in Fig. 10.

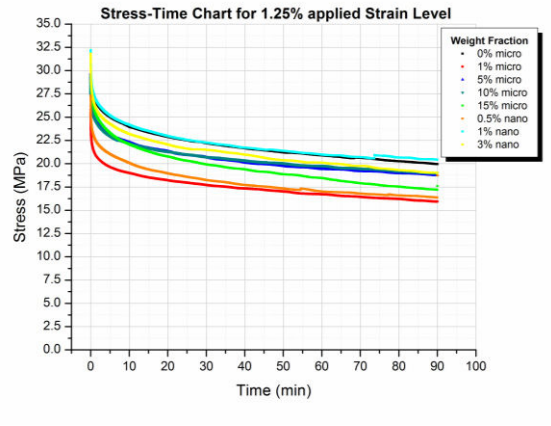

Fig. 8. Stress versus time relaxation curves, for 1.25% applied strain level, and for different TiO_2 particle sizes and weight fractions.

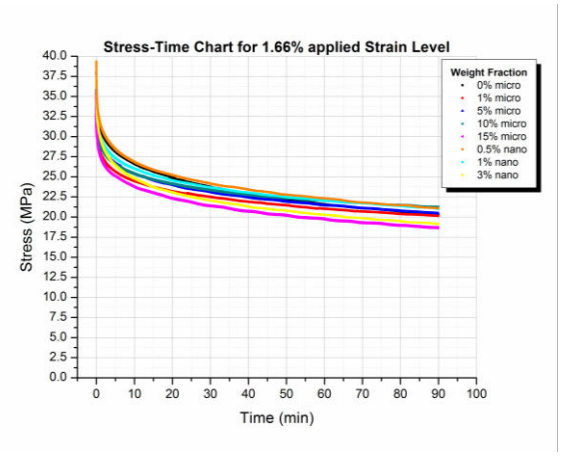

Fig. 9. Stress versus time relaxation curves, for 1.66% applied strain level, and for different TiO_2 particle sizes and weight fractions.

5.5. Application of viscoelastic models

In order to describe and/or predict the viscoelastic behaviour of the materials manufactured two viscoelastic models where applied. The first one is the Burger's model and it was applied on the creep-recovery experimental results (Fig. 11), and the second one is the Residual Property Model and it was applied on the stress relaxation results (Fig. 12-14).

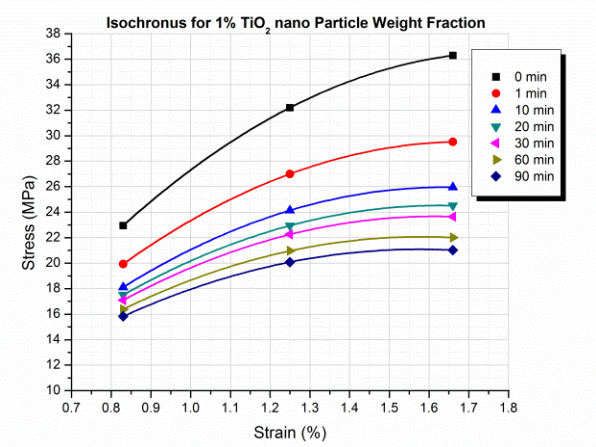

Fig. 10. Isochronous curves of epoxy-TiO_2 nano-composite with 1%wt particle concentration at different applied strain levels up to 1.66%.

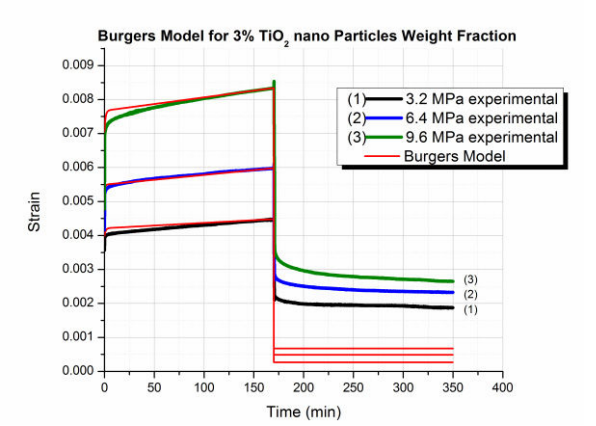

Fig. 11. Comparison between creep-recovery experimental behaviour and respective values as derived by the Burger's model application for the epoxy-TiO_2 nano-composites with 3%wt particle concentration.

Burger's model is a descriptive model based on the Boltzmann Superposition Principle, which means that is better suited to describe linear viscoelastic behaviour. Despite that fact, and although we have entered the non-linear viscoelastic region as seen by the isochronous curves in Fig. 6, Burger's model, surprisingly, was able to describe the creep behaviour of our materials (Fig. 10). However, the model was not able to describe the recovery behaviour due to the plastic deformations of the materials, as expected.

Next, taking into account that the applied strain levels for studying the viscoelastic relaxation behaviour of our materials are too high and the materials undergo plastic deformation even at the lowest strain level, RPM model using only two experimental points, predicts fairly well the obtained experimental data (Fig. 12-14).

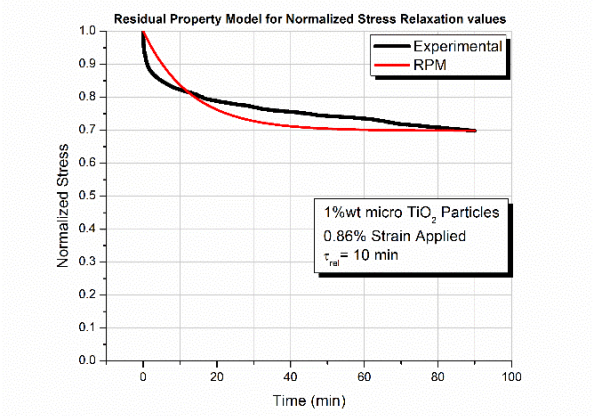

Fig. 12. Comparison between normalized relaxation experimental values and Residual Property Model (RPM) predictions for epoxy-TiO_2 micro- composites with 1%wt particle concentration (0.86% strain applied).

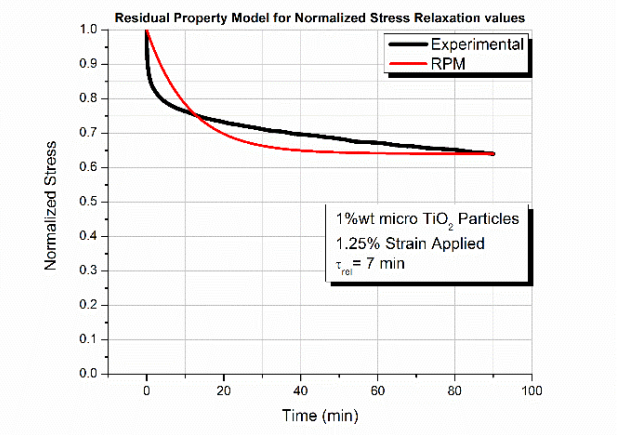

Fig. 13. Comparison between normalized relaxation experimental values and Residual Property Model (RPM) predictions for epoxy-TiO_2 micro- composites with 1%wt particle concentration (1.25% strain applied).

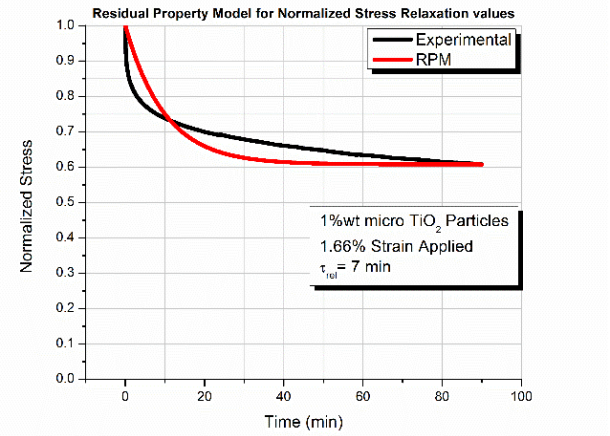

Fig. 14. Comparison between normalized relaxation experimental values and Residual Property Model (RPM) predictions for epoxy-TiO_2 micro- composites with 1%wt particle concentration (1.66% strain applied).

This is confirmed from the deviations between experimental points and respected predictions calculated in Table 2.

Table 2. Deviation between experimental values and RPM predictions.

Time(min) / ε_0	0.86% Applied Strain	1.25% Applied Strain	1.66% Applied Strain
1	0.074	0.119	0.114
10	0.014	0.020	0.009
20	0.026	0.034	0.040
30	0.042	0.048	0.052
40	0.043	0.047	0.046
50	0.038	0.039	0.037
60	0.034	0.029	0.025
70	0.018	0.019	0.016
80	0.009	0.011	0.006
90	2.8E-4	9.6E-5	4.3E-5

At this point, it is worth to mention that RPM model was developed for the prediction of the residual elastic or linear viscoelastic behaviour after damage while in present case the relaxation behaviour due to the high strain levels applied is non-linear viscoelastic.

6. Conclusions

The present study investigated the effect of the size of TiO_2 micro- and nano-particles on the quasi-static mechanical and viscoelastic properties of epoxy/TiO_2 composites. Theoretical models were also applied in order to describe and/or predict the experimental results. The Property Prediction Model (PPM), which is developed by the first author, was applied in order to predict the variation of the tensile modulus as a function of the filler volume fraction. Also, for the viscoelastic behaviour, Burger's model was applied on creep-recovery experimental findings. Finally, the RPM model, which was also developed by the first author, was applied on the stress relaxation results. From the whole work, the following conclusions can be derived:

- The grain size affects the behaviour of the tensile modulus, since the increase of the tensile modulus in nano-composites is steeper. That can be attributed to the nano- TiO_2 particles higher contact surface area.
- The Property Prediction Model (PPM) was applied on the quasi-static tensile results and predicted perfectly the variation of the tensile modulus of both micro- and nano- epoxy/TiO_2 composites.
- From the application of the same model a medium degree of adhesion K (0.33 for the nano- and 0.56 for the micro-composites) was calculated. However, the model predicts a value of 0.48 for the degree of dispersion, L, for the micro-composites while it predicts a very high degree of dispersion for the nano-composites (L=0.95).These findings also confirm our experimental observations through SEM photomicrographs.
- The grain size affects the viscoelastic behaviour of the composites tested, however the difference between micro- and nano- composites behaviour decreases as the applied excitation level (stress/strain) increases. At very high levels of excitation it appears as if the particles diameter does not affect the viscoelastic creep/relaxation behaviour of the composites manufactured.
- Finally, the viscoelastic behaviour of our materials is described fairly well by the RPM model, even though the specimens have entered the non-linear viscoelastic region, as concluded by the isochronous curves. But most importantly the model manages to predict the relaxation behaviour of our materials using only two experimental points.

References

[1] A. Chatterjee, M.S. Islam, Mater. Sci. Eng., A, 487 (2008) 574.

[2] C. Chen, R.S. Justice, D.W. Schaefer, J.W. Baur, Polymer 49 (2008) 3805.

[3] J. Baller, N. Becker, M. Ziehmer, M. Thomassey, B. Zielinski, U. Muller, R. Sanctuary, Polymer 50 (2009), 3211.

[4] R. Zhao, W. Luo, Mater. Sci. Eng., A, 483-484 (2008) 313.

[5] Y. Zheng, Y. Zheng, R. Ning, Mater. Lett. 57 (2003), 2940.

[6] V. Kostopoulos, A. Baltopoulos, P. Karapappas, A. Vavouliotis, A. Paipetis, Compos. Sci. Technol. 70 (2010) 553.

[7] J. Leidner, R. T. Woodhams, J. Appl. Polym. Sci. 18 (1974) 1639.

[8] A.N. Gent, B. Park, J. Mater. Sci. 19 (1984) 1947.

[9] K. C. Radford, J. Mater. Sci. 6 (1971) 1286.

[10] Y. Nakamura, M. Yamaguchi, M. Okubo, T. Matsumoto, J. Appl. Polym. Sci. 44 (1992) 151.

[11] N. Suprapakorn, S.S. Dhamrongvaraporn, H. Ishida, Polym. Compos. 19 (1998) 26.

[12] Z.K. Zhu, Y. Yang, J. Yin, Z.N. Qi, J. Appl. Polym. Sci. 73 (1999) 2977.

[13] J. Cho, M.S. Joshi, C.T. Sun, Compos. Sci. Technol. 66 (2006) 1941.

[14] X.L. Ji, J.K. Jing, B.Z. Jiang, Polym. Eng. Sci. 42 (2002) 983

[15] J. Douce, J.P. Boilot, J. Biteau, L. Scodellaro, A. Jimenez, Thin Solid Films 466 (2004) 114

[16] S. Mishra, S.H. Sonawane, R.P. Singh, J. Polym. Sci., Part B: Polym. Phys. 43 (2005) 107

[17] S.-Y. Fu, X.-Q. Feng, L. Bernd, Y.-W. Mai, Composites, Part B 39 (2008) 933

[18] L. Cano, J. Gutierrez, A. E. Di Mauro, M.L. Curri, A. Tercjak, Electrochim. Acta 184 (2015) 8.

[19] Y. Li, J. Luo, X. Hu, X. Wang, j> Liang, K. Yu, J. Alloys Compd. 651 (2015) 685.

[20] A.I. Kociubczyk, M.L. Vera, C.E. Schvezov, E. Heredia, A.E. Ares, Procedia Mater. Sci. 8 (2015) 351.

[21] C.D. Madhusoodana, S.P. Manjunath, R.N. Das, Procedia Eng. 44 (2012) 939.

[22] T. Plecenik, M. Mosko, A.A. Haidry, P.Durina, M. Truchly, B. Grancic, M. Gregor, T. Roch, L. Satrapinskyy, A. Moskova, M. Mikula, P. Kus, A. Plecenik, Sens. Actuators, B 207 (2015) 351.

[23] K. Choi, W. Lee, Ch. Lim, Mater. Lett. 158 (2015) 36.

[24] K.G. Binu, B.S. Shenoy, D.S. Rao, R. Pai, Procedia Mater. Sci. 6 (2014) 1051.

[25] A. Purniawan, P.J. French, G. Pandraud, P.M. Sarro, Procedia Eng. 5 (2010) 1131.

[26] C.B. Ng, L.S. Schadler, R.W. Siegel, Nanostruct. Mater. 12 (1999) 507.

[27] H.A. Al-Turaif, Prog. Org. Coat. 69 (2010) 241.

[28] M. Kosmulski, Surface charging and points of zero charge, CRC Press: Boca Raton, FL, 2009.

[29] G.C. Papanicolaou, A.F. Koutsomitopoulou, A. Sfakianakis, J. Appl. Polym. Sci. 124 (2011) 67.

[30] G.C. Papanicolaou, L.C. Kontaxis, A.F. Koutsomitopoulou, S.P. Zaoutsos, J. Appl. Polym. Sci. 132 (2015) 41697

[31] F. Rabbi, PhD thesis, (2014) Retrieved from http://scholarcommons.sc.edu/etd/2868

[32] G.C. Papanicolaou, T.V. Kosmidou, A.S Vatalis, C.G. Delides, J. Appl. Polym. Sci. 99 (2006) 1328.

[33] G.C. Papanicolaou, A.G. Xepapadaki, G.A. Angelakopoulos, J. Appl. Polym. Sci. 126 (2012) 559.